symmetry

MDPI

Review

Nuclear Shape-Phase Transitions and the Sextic Oscillator

Géza Lévai [1,*] and José M. Arias [2,3]

[1] HUN-REN Institute for Nuclear Research (ATOMKI), P.O. Box 51, H-4001 Debrecen, Hungary
[2] Departamento de Física Atómica, Molecular y Nuclear, Facultad de Física, Universidad de Sevilla, Apartado 1065, 41080 Sevilla, Spain; ariasc@us.es
[3] Instituto Carlos I de Física Teórica y Computacional, Universidad de Granada, Fuentenueva s/n, 18071 Granada, Spain
* Correspondence: levai@atomki.hu

Abstract: This review delves into the utilization of a sextic oscillator within the β degree of freedom of the Bohr Hamiltonian to elucidate critical-point solutions in nuclei, with a specific emphasis on the critical point associated with the β shape variable, governing transitions from spherical to deformed nuclei. To commence, an overview is presented for critical-point solutions E(5), X(5), X(3), Z(5), and Z(4). These symmetries, encapsulated in simple models, all model the β degree of freedom using an infinite square-well (ISW) potential. They are particularly useful for dissecting phase transitions from spherical to deformed nuclear shapes. The distinguishing factor among these models lies in their treatment of the γ degree of freedom. These models are rooted in a geometrical context, employing the Bohr Hamiltonian. The review then continues with the analysis of the same critical solutions but with the adoption of a sextic potential in place of the ISW potential within the β degree of freedom. The sextic oscillator, being quasi-exactly solvable (QES), allows for the derivation of exact solutions for the lower part of the energy spectrum. The outcomes of this analysis are examined in detail. Additionally, various versions of the sextic potential, while not exactly solvable, can still be tackled numerically, offering a means to establish benchmarks for criticality in the transitional path from spherical to deformed shapes. This review extends its scope to encompass related papers published in the field in the past 20 years, contributing to a comprehensive understanding of critical-point symmetries in nuclear physics. To facilitate this understanding, a map depicting the different regions of the nuclide chart where these models have been applied is provided, serving as a concise summary of their applications and implications in the realm of nuclear structure.

Keywords: nuclear structure models and methods; collective models; Bohr Hamiltonian; quasi-exactly solvable models; sextic potential

PACS: 21.60.-n; 21.60.Ev; 21.60.Fw

Citation: Lévai, G.; Arias, J.M. Nuclear Shape-Phase Transitions and the Sextic Oscillator. *Symmetry* **2023**, *15*, 2059. https://doi.org/10.3390/sym15112059

Academic Editors: Peter Otto Hess and Charalampos Moustakidis

Received: 14 October 2023
Revised: 28 October 2023
Accepted: 10 November 2023
Published: 14 November 2023

1. Introduction

Phase transitions are typically well-defined and associated with macroscopic systems [1]. However, in recent years, early indicators of phase transitions have been observed in mesoscopic systems [2], leading to the concept of quantum phase transitions [3,4]. In classical physics, phase transitions are traditionally classified into two categories: first-order and continuous phase transitions, based on the behavior of the order parameter at the critical point. At this juncture, the order parameter typically undergoes a discontinuous change from zero to a finite value in first-order transitions, whereas in continuous transitions, the change is smooth at the critical point. These same principles apply to quantum phase transitions. It is evident that the notion of a critical point is closely intertwined with the study of phase transitions.

An intriguing facet of modern nuclear physics involves the exploration of the quantum shape-phase transition (QSPT) in atomic nuclei. In this context, QSPTs have been studied in nuclear physics with the introduction of shape variables. Different shape phases imply different spectral patterns (energy spectrum, electromagnetic transitions, etc.), and often different symmetries. The transitions from one shape phase to another thus correspond to structural rearrangements in the nucleus. Identifying these is thus of primary importance in understanding certain aspects of nuclear structure. The Bohr Hamiltonian was developed to capture the dynamics of quadrupole-type surface excitations in nuclei [5]. It relies on two key variables: $\beta \geq 0$, which quantifies the deviation of the nuclear surface from a spherical shape, and $\gamma \in [0, \pi/3]$, which characterizes its deviation from axial symmetry. In addition, describing the orientation of the nucleus requires Euler angles, rendering the problem in a five-dimensional space. The kinetic term encompasses all five variables, whereas the potential depends solely on the intrinsic β and γ shape variables. The position of the potential minimum dictates the nuclear shape, which could be spherical, deformed prolate, deformed oblate, deformed triaxial, deformed γ-unstable, and so forth. Changes in a control parameter in the Hamiltonian can produce a transition from one specific form to another. The point of change is called a critical point and is characterized by a critical value of the appropriate control parameter. In the context of the Bohr Hamiltonian [5], a few decades ago, Iachello introduced the concept of critical-point symmetries concerning quantum systems like atomic nuclei [6]. Iachello formulated two critical-point symmetries within the geometric model. One of these symmetries, known as E(5), characterizes the critical point in the shape transition from spherical to deformed γ-unstable shapes [6] and is particularly relevant for describing continuous shape-phase transitions. Another symmetry proposed by Iachello, referred to as X(5), pertains to the critical point in the transition from spherical to axially deformed shapes [7] and serves as a benchmark for first-order phase transitions. In addition to these critical points, Iachello also discussed a phase transition in the angle variables [8] and particularized the phase transition from axial to triaxial shapes in nuclei. The corresponding critical point is known as Y(5). Soon after, Bonatsos and collaborators proposed a model for the critical point in the transition from oblate to prolate shapes, approximately separating variables in the Bohr Hamiltonian for $\gamma = \pi/6$ [9]. This critical point is called Z(5). Some other critical-point solutions, such as X(3) and Z(4), have been proposed and are discussed below.

Another widely employed nuclear structure model for exploring shapes and shape-phase transitions is the Interacting Boson Model (IBM) [10]. While the IBM was originally formulated within a second quantization formalism, it is possible to gain a geometric understanding of the model by leveraging the concept of coherent states and the intrinsic state formalism [11–13]. This approach unveils geometric shapes, akin to the Bohr model, which are associated with the various dynamical symmetries of the IBM. These correspond to special situations in which exact analytical solutions of the many-body problem can be obtained using group theory techniques. These dynamical symmetries are labeled as U(5), SU(3) ($\overline{\text{SU(3)}}$), and O(6). With the introduction of shape variables, the U(5) limit corresponds to spherical shapes, the SU(3) ($\overline{\text{SU(3)}}$) limit yields prolate (oblate) axially symmetric shapes, and the O(6) limit generates deformed γ-unstable shapes. This prompts the search for counterparts to the E(5) and X(5) symmetries within the IBM. In this context, the critical points are referred to as $e(5)$ and $x(5)$, respectively, and they represent the transitional pathways from U(5) to O(6) and from U(5) to SU(3). Significant experimental and theoretical investigations have been conducted to explore quantum phase transitions, particularly for even-even nuclei within the IBM, as documented in various reviews [14–18].

The introduction of critical-point symmetries has sparked a quest to identify nuclei that align with the predictions of these models. Additionally, it has spurred investigations into potentials that yield exact solutions within the Bohr Hamiltonian framework (for a comprehensive review, please refer to Ref. [19]). Our contribution to these endeavors includes the proposal of the sextic oscillator potential for the β shape variable, making the potential energy surface independent of γ [20–23]. This potential exhibits remarkable flexibility: its characteristics can vary depending on the parameters, featuring either a spherical minimum, a deformed minimum, or both. Moreover, the transition between these different shape phases can be controlled analytically. The sextic oscillator belongs to the category of quasi-exactly solvable (QES) potentials [24,25], implying that only the lowest few energy levels can be obtained exactly. Fortunately, these few lowest energy levels generally correspond to the set of nuclear states for which a sufficient amount of experimental spectroscopic information is available, allowing for a quantitative comparison of experiment and theory. We have also derived electromagnetic transition rates ($B(E2)$, $B(E0)$) for this potential in closed form and computed benchmark values associated with the transitions between different shape phases [21–23].

During the last 15 years, a systematic investigation of the quantum shape-phase transitions linked to the sextic potential has been developed. Many works have employed the sextic oscillator in the Bohr Hamiltonian with potentials dependent on the γ shape variable. Various nuclear shapes have been explored, including γ-stable triaxial [26], γ-stable prolate [27], γ-rigid triaxial [28], and γ-rigid prolate [29] nuclei (for an extensive review from 2015, see Ref. [30]). Numerical investigations for the sextic oscillator have also been conducted to describe double-well structures [31]. An examination of higher QES solutions of the sextic oscillator [32] concluded that solutions with up to two nodes appear to be the most suitable approximation for studies on phase transitions. Applications to different regions of the nuclear chart table have been reported with all these approaches.

In this review, we present a summary of the most important results obtained in the past 20 years in the framework of the Bohr equation solved with a sextic potential in the β degree of freedom. This material is organized as follows. In Section 2, the Bohr Hamiltonian is revisited, and its solutions with a γ-independent sextic oscillator in the β variable are described. In Section 3, other various solutions of the Bohr Hamiltonian with a sextic potential in the β variable are discussed, including several ways of treating the angular variable γ. Some general conclusions are drawn in Section 4.

2. The Bohr Hamiltonian

The Bohr Hamiltonian describes the collective motion of the nucleus as a five-dimensional system. The deformation variable β measures the deviation from the spherical shape, whereas γ accounts for the deviation from axial symmetry toward triaxial configurations. The remaining three variables are the three Euler angles ($\theta_1, \theta_2, \theta_3$), which describe the spatial orientation of the deformed nucleus. After separating the angular variables, the Bohr Hamiltonian is written as follows [5]:

$$H = -\frac{\hbar^2}{2B}\left[\frac{1}{\beta^4}\frac{\partial}{\partial\beta}\beta^4\frac{\partial}{\partial\beta} + \frac{1}{\beta^2 \sin 3\gamma}\frac{\partial}{\partial\gamma}\sin 3\gamma\frac{\partial}{\partial\gamma} - \frac{1}{4\beta^2}\sum_k \frac{Q_k^2}{\sin^2(\gamma - \frac{2}{3}\pi k)}\right] + V(\beta,\gamma), \quad (1)$$

where B is the mass parameter and $Q_k (k = 1, 2, 3)$ are the components of the angular momentum in the intrinsic reference frame. It is worthwhile switching to reduced energies by rescaling the energy and potential terms as $\epsilon = \frac{2B}{\hbar^2}E$ and $v(\beta,\gamma) = \frac{2B}{\hbar^2}V(\beta,\gamma)$, respectively. Note that the deformation variable β is dimensionless, and so are $v(\beta,\gamma)$ and ϵ. The mass parameter B appears as a moment of inertia, and as such, it has the physical dimension $mass \times length^2$. Its chosen value sets the energy scale [23].

In order to solve the two-dimensional partial differential Equation (1), one usually has to apply various assumptions and approximations. The problem can be simplified if we assume that the potential has a separable form:

$$v(\beta,\gamma) = u(\beta) + \frac{w(\gamma)}{\beta^2}. \quad (2)$$

In this case, the terms with the γ variable can be separated into a second-order differential operator containing the differential terms and $w(\gamma)$. By solving the corresponding differential equation, the resulting eigenvalues then appear in the β-differential equation together with the β^{-2} factor.

The electric quadrupole transitions are calculated using the first-order transition operator [5,6,33]

$$T^{(\mathrm{E2})} = t\beta\left[D^{(2)}_{\mu,0}(\theta_i)\cos\gamma + \frac{1}{\sqrt{2}}\left(D^{(2)}_{\mu,2}(\theta_i) + D^{(2)}_{\mu,-2}(\theta_i)\right)\sin\gamma\right], \tag{3}$$

where $D^{(j)}_{m,m'}(\theta_i)$ are rotation Wigner D-matrices, and t is a scale parameter. In some situations, this operator may impose overly restrictive selection rules. These can be relaxed by adding a second-order term to (3), where t' is an additional parameter:

$$T^{(\mathrm{E2})\prime} = T^{(\mathrm{E2})} + t'\beta^2\left[-D^{(2)}_{\mu,0}(\theta_i)\cos(2\gamma) + \frac{1}{\sqrt{2}}\left(D^{(2)}_{\mu,2}(\theta_i) + D^{(2)}_{\mu,-2}(\theta_i)\right)\sin(2\gamma)\right]. \tag{4}$$

The B(E2) electric quadrupole transition rates can be calculated as the matrix elements of operators (3) or (4).

2.1. Special Solvable Cases and Critical-Point Symmetries

Several special cases have been discussed for which exact solutions can be obtained. These cases are based on further assumptions or approximations that simplify the mathematical formalism. Most of these are associated with various symmetries. Typically, these special cases have been introduced using the infinite square well as $u(\beta)$ in (2), the flat bottom of which is considered an approximation of the shape-phase transition between two potential minima (see, e.g., Ref. [6] for details). Here, we briefly review these models, keeping in mind that they can also be implemented using the sextic oscillator as $u(\beta)$. In some of these models, the γ degree of freedom is omitted ($w(\gamma) = 0$) or γ is restricted to a constant value, reducing the Bohr Hamiltonian to the Davydov–Chaban Hamiltonian [34]. These models are technically less involved, allowing for exact solutions. In others, $w(\gamma)$ is approximated with some simple potential.

$E(5)$ symmetry: A special case arises for γ-unstable potentials, which depend explicitly only on the β variable, i.e., $w(\gamma) = 0$ in (2). Then, the β-dependence can be separated into an equation similar to the radial Schrödinger equation by using the substitution,

$$\Psi(\beta, \gamma, \theta_i) = \beta^{-2}\phi(\beta)\Phi(\gamma, \theta_i). \tag{5}$$

The β-differential equation is then

$$-\frac{d^2\phi(\beta)}{d\beta^2} + \left[\frac{(\tau+1)(\tau+2)}{\beta^2} + u(\beta)\right]\phi(\beta) = \epsilon\phi(\beta). \tag{6}$$

Here, τ is the seniority quantum number, which determines the allowed L angular momentum values (see Section 2.2). By taking the infinite square well as $u(\beta)$, this model is associated with the $E(5)$ symmetry describing the transition between the spherical and the deformed γ-unstable shape phases [6].

$X(5)$ symmetry: This model describes the transition from the spherical to axially deformed shape phases. Here, the collective Hamiltonian is the original Bohr Hamiltonian in five dimensions. This case corresponds to the situation in which the potential is separable, $v(\beta, \gamma) = u(\beta) + \tilde{w}(\gamma)$, where the β^2 factor in Equation (2) is approximated using its mean value $\langle\beta^2\rangle$. In this situation, the differential equation is approximately separable in the variables β and γ. Then, a harmonic oscillator with a minimum at $\gamma = 0$ is used for the γ degree of freedom, whereas for the potential in β, an infinite square well is assumed [7].

$Z(5)$ symmetry: This model accounts for the prolate to oblate shape-phase transition. In this case, the variables in the Bohr Hamiltonian are approximately separated for $\gamma = \pi/6$. A harmonic oscillator potential with a minimum at $\gamma = \pi/6$ in the γ variable was proposed, whereas for the β variable, an infinite square well was assumed [9].

$X(3)$ symmetry: This is a γ-rigid (with $\gamma = 0$) version of the $X(5)$ model. It is called $X(3)$ because only three variables occur in this case, and the separation of variables is exact. The collective Hamiltonian (in reduced units) is given in this case by

$$h = -\frac{1}{\beta^2}\frac{\partial}{\partial\beta}\beta^2\frac{\partial}{\partial\beta} - \frac{Q^2}{3\beta^2} + v(\beta,\gamma). \tag{7}$$

This is the case when γ is not considered as a variable but rather as a parameter with a given value (γ-rigid case), such as $\gamma = 0$. For the β variable, an infinite square well is also assumed [35].

$Z(4)$ symmetry: This is another γ-rigid version but in this case, of Z(5). γ is considered as a parameter fixed to $\gamma = \pi/6$ (not a variable). In this situation, the Bohr equation is a function of four variables (β and the Euler angles). The Bohr Hamiltonian splits into two equations: one for the β variable and another for the Euler angles

$$\left[\frac{1}{\beta^3}\frac{\partial}{\partial\beta}\beta^3\frac{\partial}{\partial\beta} - \frac{\lambda}{\beta^2} + (\epsilon - u(\beta))\right]\phi(\beta) = 0 \;\; ; \;\; \left[\frac{1}{4}\sum_{k=1}^{3}\frac{Q_k^2}{\sin^2(\gamma - \frac{2\pi k}{3})} - \lambda\right]\Phi)\theta_i) = 0, \tag{8}$$

where ϵ and u are the reduced energies and potentials introduced previously, and θ_i (i = 1, 2, 3) are the Euler angles. For $\gamma = \pi/6$, the angular equation was solved long ago by Meyer-ter-Vehn [36], with $\lambda = \lambda_{L,\alpha} = L(L+1) - 3\alpha^2/4$, where α are the eigenvalues of the projection of the angular momentum on the body-fixed axis and are even integers [36]. For the β variable, an infinite square well is used here too [37].

All these critical-point solutions are summarized in Figure 1.

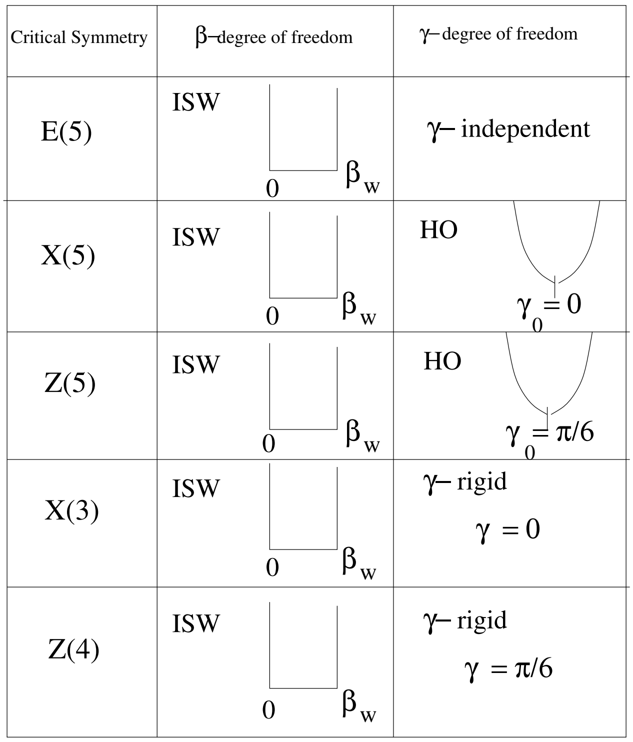

Figure 1. Pictorial summary of the critical-point solutions in the β degree of freedom.

2.2. *The Sextic Oscillator as* $u(\beta)$

The solutions of the general sextic oscillator

$$u_6(r) = A_{-2}r^{-2} + A_0 + A_2r^2 + A_4r^4 + A_6r^6\;, \tag{9}$$

cannot be written in an exact form. However, some of its special subsets admit partial exact solutions. In this case, the A_i coefficients satisfy certain constraints. This happens for the quasi-exactly solvable (QES) subset of the sextic oscillator [24], both as a radial ($r \in [0, \infty)$, $A_{-2} \neq 0$) and as a one-dimensional ($x \in (-\infty, \infty)$, $A_{-2} = 0$) problem. Choosing the former with $r = \beta \in [0, \infty)$ and incorporating the β^{-2} term from Equation (6) using $A_{-2} = (\tau + 1)(\tau + 2)$, the normalizable solutions are written in terms of an infinite power series of β^2 multiplied by a suitable pre-factor containing exponential forms of β^2 and β^4. Substituting it into the Schrödinger equation and collecting the terms with the same powers β^{2i}, its coefficients are found to satisfy an infinite three-term recurrence relation. However, the recursion can be terminated by a suitable choice of the parameters, leading to a polynomial form, $P^{(M)}(\beta^2)$, of the solutions:

$$\phi(\beta) \sim \beta^{\tau+2} \exp\left[-\frac{a}{4}\beta^4 - \frac{b}{2}\beta^2\right] P^{(M)}(\beta^2) \,, \tag{10}$$

where a and b are model parameters defining the β potential (see below). In this way, the first $M + 1$ normalizable solutions can be obtained in closed form. Note that for $A_6 > 0$, the sextic oscillator tends to infinity asymptotically, so it has an infinite number of bound states. The termination condition leads to constraints on the coefficients of the potential terms, so eventually, the QES sextic oscillator potential takes the form

$$u(\beta) = u^{\pi}(\beta) = (b^2 - 4ac^{\pi})\beta^2 + 2ab\beta^4 + a^2\beta^6 + u_0^{\pi} \,. \tag{11}$$

Here, a and b are the parameters appearing in the exponential term of $\phi(\beta)$ in Equation (10). The $a = 0$ choice recovers the harmonic oscillator. c^{π} is a constant that is determined by τ and M as

$$2c^{\pi} = \tau + 2M + \frac{7}{2} \,. \tag{12}$$

It is worth noting that all these conditions are necessary to obtain a QES potential with state-independent exact analytical solutions. Relation (12) implies that the normalizable solutions of the QES sextic oscillator are composed of $\phi(\beta)$ functions (10) with all combinations of τ and M for which $\tau + 2M = const$. It is obvious that c^{π} differs for τ-even (c^+) and τ-odd (c^-) combinations, which also introduces a slight difference in the coefficient of the quadratic potential component. This effect, which proved to be marginal in the applications in [20–23], was handled by prescribing that the minima of the two potentials coincide. This can be achieved by applying different constants in potential (11). For $M = 2$, these constants are:

$$u_0^+ = 0, \tag{13}$$

$$u_0^- = \begin{cases} (b^2 - 15a)(\beta_0^+)^2 - (b^2 - 17a)(\beta_0^-)^2 & \\ +2ab[(\beta_0^+)^4 - (\beta_0^-)^4] + a^2[(\beta_0^+)^6 - (\beta_0^-)^6] \,; & \text{if} \quad b < (15a)^{\frac{1}{2}} \\ -(b^2 - 17a)(\beta_0^-)^2 - 2ab(\beta_0^-)^4 - a^2(\beta_0^+)^6 \,; & \text{if} \quad (15a)^{\frac{1}{2}} < b < (17a)^{\frac{1}{2}} \\ 0 \,; & \text{if} \quad b > (17a)^{\frac{1}{2}} \end{cases} \tag{14}$$

where

$$\beta_0^{\pi} = \frac{1}{3a}[-2b \pm (b^2 + 12ac^{\pi})^{\frac{1}{2}}] \,. \tag{15}$$

See Refs. [20–23] for the detailed calculations.

The parameter space (a, b) is divided into three characteristic domains, each corresponding to a specific potential shape in Figure 2. On the right of the parabola $a = b^2/(4c^{\pi})$, the coefficients of both the β^2 and β^4 potential terms are positive, so the $u(\beta)$ potential shows a monotonously increasing trend with β, and it has a minimum at $\beta_0 = 0$. Above the parabola, the coefficient of the quadratic term is negative, so the potential has a local maximum at $\beta_0 = 0$ and a minimum at $\beta_1 > 0$. Finally, on the left of the parabola, the coefficients of the quadratic and quartic terms are positive and negative, respectively, resulting in a local minimum at $\beta_0 = 0$, a local maximum at $\beta_1 > 0$, and another minimum at $\beta_2 > \beta_1$. It can be proven that the latter minimum is always deeper than that located at $\beta_0 = 0$. Potentials corresponding to parameters lying on the parabola lack the quadratic term, so they have a relatively flat bottom near $\beta = 0$. This situation is close to the infinite square well, which has been considered as the model of phase transition from the spherical to the axially deformed minimum in γ-unstable nuclei with $E(5)$ symmetry. It has been shown [20,21] that various benchmark numbers (ratios of energy eigenvalues or electric quadrupole transition rates) are constant along the parabola.

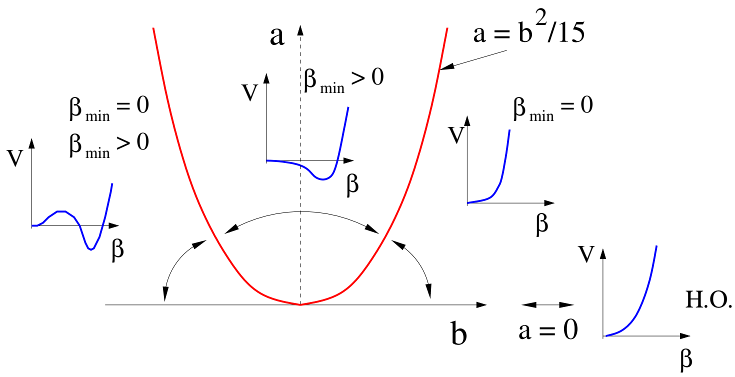

Figure 2. Sextic model space (a, b) and the corresponding energy surfaces $u(\beta)$ (11) in the different regions for M = 2, which corresponds to $c^+ = 15/4$ and $c^- = 17/4$. The parabola $a = b^2/15$ separates spherical from deformed shapes for $b > 0$ and deformed shapes from a coexistence region with two minima: one spherical and another deformed ($b < 0$). The figure was taken from Ref. [22] and is licensed under CC BY-SA 4.0.

Before proceeding, we note that the sextic oscillator can also be formally obtained through a suitable transformation from the bi-confluent Heun equation. In particular, the polynomial solutions of this equation coincide with the QES solutions of the sextic oscillator (see [38] for details on the relation between the two approaches).

Once the potential $u(\beta)$ in Equation (11) has been selected, i.e., a, b, and c^π are fixed, the energy eigenvalues and eigenstates can be determined. For this, the eigenvalues of the $(M+1) \times (M+1)$ matrix (obtained from the termination of the three-term recurrence relation) have to be diagonalized. This amounts to finding the roots of an $(M+1)$'th-degree algebraic equation. This has to be carried out for each M and τ satisfying prescription (12). This task can be completed numerically; however, for $M = 0$, 1, and 2, the roots can be obtained in closed analytic form. In the first publications proposing the application of the sextic oscillator in the Bohr Hamiltonian [20,21], solutions up to $M = 1$ were considered, and the energy eigenvalues and eigenstates were determined in closed analytical form. Later, the formalism was extended up to $M = 2$ [22], which extended the basis to 30 states (from 10), with nodal excitation up to $\xi = 3$ (from 2) and angular momentum up to $L = 10$ (from 6). For this, the roots of a cubic algebraic equation had to be calculated in the standard way. Here, we briefly recall the essential formulas for the energy eigenvalues and refer to Ref. [22] for any further expressions (coefficients appearing in the polynomial solutions, integrals appearing in the matrix elements, etc.).

The energy eigenvalues are determined for τ-even and τ-odd states separately. According to Equation (12), the choice $\tau + 2M = 4$, which allows combinations such as $\tau = 0$, $M = 2$; $\tau = 2$, $M = 1$; and $\tau = 4$, $M = 0$, corresponds to $c^+ = 15/4$. Similarly, $\tau + 2M = 5$ includes combinations such as $\tau = 1$, $M = 2$; $\tau = 3$, $M = 1$; and $\tau = 5$, $M = 0$, corresponding to $c^- = 17/4$ [20]. This difference between c^+ and c^- also defines the difference between the τ-even and τ-odd potentials as $2a\beta^2$. The energy eigenvalues are displayed in Table 1, where the various $\lambda_i^{(M)}$ quantities are obtained from the solution of the $(M+1)$'th-order algebraic equations.

Table 1. The energy eigenvalues of the sextic oscillator adapted to the Bohr Hamiltonian [22]. The constant terms u_0^π in Equations (13) and (14) that depend on the even or odd value of τ are subtracted for simplicity. The $\lambda_i^{(M)}$ and $\tilde{\lambda}_i^{(M)}$ quantities are displayed in Equations (16) and (17). The fifth column displays the angular momenta L contained in the given (ξ, τ) multiplet.

ξ	τ	M	$\epsilon_{\xi,\tau} - u_0^\pi$	L
1	0	2	$\begin{cases} \lambda_2^{(2)}; & b > 0, \\ \lambda_1^{(2)}; & b < 0, \end{cases}$	0
1	2	1	$9b + \lambda_-^{(1)}$	2, 4
1	4	0	$5b + \lambda_3^{(2)}$	2, 4, 5, 6, 8
2	0	2	$5b + \lambda_3^{(2)}$	0
2	2	1	$9b + \lambda_+^{(1)}$	2, 4
3	0	2	$5b + \begin{cases} \lambda_1^{(2)}; & b > 0, \\ \lambda_2^{(2)}; & b < 0, \end{cases}$	0
1	1	2	$7b + \begin{cases} \tilde{\lambda}_2^{(2)}; & b > 0, \\ \tilde{\lambda}_1^{(2)}; & b < 0, \end{cases}$	2
1	3	1	$11b + \tilde{\lambda}_-^{(1)}$	0, 3, 4, 6
1	5	0	$15b$	2, 4, 5, 6, 7, 8, 10
2	1	2	$7b + \tilde{\lambda}_3^{(2)}$	2
2	3	1	$11b + \tilde{\lambda}_+^{(1)}$	0, 3, 4, 6
3	1	2	$7b + \begin{cases} \tilde{\lambda}_1^{(2)}; & b > 0, \\ \tilde{\lambda}_2^{(2)}; & b < 0, \end{cases}$	2

When introducing $s = (2\tau + 5)/4$, the quantities shown in Table 1 become the following [22]:

$$\begin{aligned} \lambda_\pm^{(1)} &= 2b \pm 2(b^2 + 18a)^{\frac{1}{2}} , \\ \tilde{\lambda}_\pm^{(1)} &= 2b \pm 2(b^2 + 22a)^{\frac{1}{2}} , \end{aligned} \tag{16}$$

$$\begin{aligned} \lambda_i^{(2)} &= \Lambda_i^{(2)}(5/4) , \quad s = 5/4 \text{ for } \tau = 0 \\ \tilde{\lambda}_i^{(2)} &= \Lambda_i^{(2)}(7/4) , \quad s = 7/4 \text{ for } \tau = 1 \end{aligned} \tag{17}$$

where

$$\begin{aligned} \Lambda_1^{(2)}(s) &= 4b - 2r\cos(\frac{\phi}{3}) , \\ \Lambda_2^{(2)}(s) &= 4b + 2r\cos(\frac{\pi}{3} - \frac{\phi}{3}) , \\ \Lambda_3^{(2)}(s) &= 4b + 2r\cos(\frac{\pi}{3} + \frac{\phi}{3}) , \\ \cos(\phi) &= -\frac{64ab}{r^3} , \\ r &\equiv r(s) = \pm\left[\frac{16}{3}(b^2 + 2a(4s+1))\right]^{\frac{1}{2}} , \end{aligned} \tag{18}$$

and the prescription $\mathrm{sgn}(r) = -\mathrm{sgn}(b)$ has to be satisfied.

The (ξ, τ) multiplets contain one or more physical states with a given L angular momentum value. The rules determining the allowed values follow from the $O(5) \supset O(3)$ decomposition: Construct $\tau = 3n_\Delta + \nu$, where $n_\Delta = 0, 1, \ldots$. Then, the allowed L values are $L = \nu, \nu + 1, \ldots, 2\nu - 2, 2\nu$ (note that the value $L = 2\nu - 1$ is missing). Table 1 displays the allowed L values for the given (ξ, τ) multiplets.

In what follows, the energy scale is redefined such that $E = 0$ corresponds to the ground-state energy. The rescaled energy eigenvalues are denoted as

$$E_{\xi,\tau} = \epsilon_{\xi,\tau} - \epsilon_{1,0} \, . \tag{19}$$

With this model, one can obtain parameter-independent values (up to a scale factor) for energies and transition probabilities at the critical point between spherical and deformed γ-unstable shapes. These benchmark numbers are summarized in Figure 3, as taken from [22] for $M = 2$.

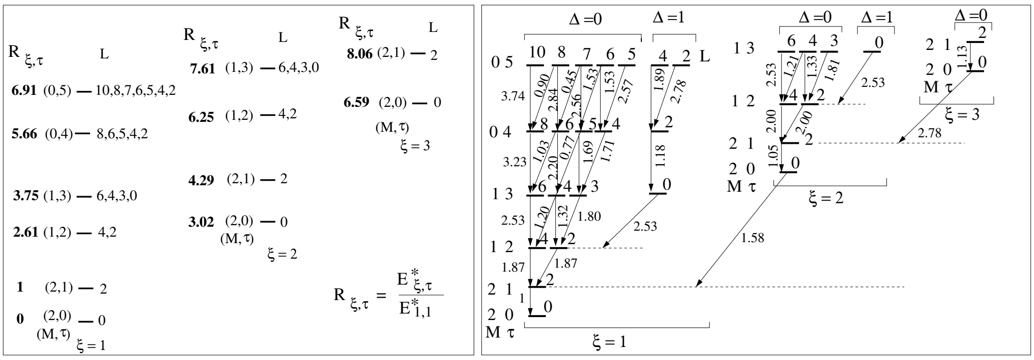

Figure 3. Benchmark numbers for energies normalized to the excitation energy of the first 2^+ (**left**) and $B(E2)$ values normalized to $B(E2; 2_1^+ \to 0_1^+) = 100$ (**right**) characterizing the transition from the spherical to the deformed domain within the sextic oscillator model. These quantities are fixed for any point of the critical parabola separating the two domains. The figures were taken from Ref. [22] and are licensed under CC BY-SA 4.0.

3. Applications of the Sextic Oscillator in the Bohr Hamiltonian

Due to its flexible shape, the sextic oscillator seems to be a suitable candidate to serve as the β-potential $u(\beta)$ in the Bohr Hamiltonian. It is the lowest-order polynomial potential that admits two minima. With a potential minimum at $\beta = 0$, it can describe spherical nuclear shapes, whereas with a minimum at $\beta > 0$, it can account for a nucleus with a deformed shape. Furthermore, the transition between the two shape phases can be implemented smoothly within an exact analytical framework simply by varying the potential parameters a and b in (11). These features have been employed in a variety of models describing a wide range of nuclear shapes and transitions between them. Several review papers have discussed solvable models within the framework of the Bohr Hamiltonian, paying special attention to the shape-phase transitions and critical-point solutions related to them [19,30,39]. In the present review, we focus on models in which the sextic oscillator was considered as the β potential and report on recent developments in the field, placing them in the context of earlier results.

3.1. $w(\gamma) = 0$

The first application of the sextic oscillator was proposed in 2004 in Ref. [20] to describe the transition between spherical and γ-unstable nuclear shapes. In this case, the γ shape variable does not play a role. Based on the corresponding critical-point symmetry, this approach can be called $E(5)$-sextic. The formalism was first developed for solutions with $M = 0$ and 1, encompassing ten states altogether: three 0^+, three 2^+, one 3^+, two 4^+, and one 6^+ levels. These model states can typically be assigned to the first four levels of the ground-state band $K^\pi = 0_1^+$, the first three levels of the quasi-γ band $K^\pi = 2^+$, and the bandheads of two further $K^\pi = 0^+$ bands.

The formalism of the sextic oscillator was developed in Ref. [20], where the energy eigenvalues, wavefunctions, and $B(E2)$ transitions were derived. The evolution of the energy spectrum was studied by varying the a and b model parameters, and the structure of the phase space was established. It was found that the phase transition occurs on the critical parabola $a = b^2/11$. This follows from selecting $c^+ = 11/4$ in Equation (12), which corresponds to $\tau + 2M = 2$, i.e., to the combinations $\tau = 0$, $M = 1$ and $\tau = 2$, $M = 0$. Closed-form benchmark numbers were calculated for the energy and $B(E2)$ ratios and were compared to the benchmark numbers of the $E(5)$ critical-point symmetry and other models. As an example, the spectroscopic data for the ^{134}Ba nucleus were calculated and compared to the experimental values.

In the next application of the model [21], the formalism was further developed: matrix elements with the $\phi(\beta)$ wave functions were calculated analytically in terms of confluent hypergeometric functions. The model was then systematically applied to the chain of even-even Ru ($A = 98$–108), Pd ($A = 102$–110), and Cd ($A = 106$–116) isotopes. The potential parameters were determined from the experimental energy eigenvalues, and the trajectories of the chains were plotted on the (a, b) phase space. Several nuclei were identified as potential critical-point candidates, i.e., those close to the critical parabola. Examples include ^{104}Ru, ^{102}Pd, ^{106}Cd, and ^{108}Cd, which were proposed previously as candidates using other models, and ^{116}Cd as a new one.

In the applications in [20,21], the key step was assigning appropriate experimental states to the excited 0^+ model states. These states have characteristic decay patterns in electric quadrupole transitions: the one denoted by $(\xi, \tau)L = (1, 3)0$ is expected to decay strongly to the second excited 2^+ state assigned to $(1, 2)2$, whereas the node-excited 0^+ state $(2, 0)0$ is expected to decay to the first excited 2^+ state $(1, 1)2$ (see Figure 3 for the notation).

Further applications of this version of the model have been presented. In Ref. [40], seven Te isotopes (from $A = 110$ to 139) and the chain of six Xe isotopes ($A = 122$–132) were discussed. All the nuclei were found to lie in the domain of a deformed minimum (above the critical parabola), with ^{110}Te closest to the position of a critical-point nucleus. In Ref. [41], the chains of Zr ($A = 88$–100) and Sn ($A = 110$–122) nuclei were investigated. Most of these nuclei were also found to belong to the domain of a deformed minimum; however, ^{96}Zr and ^{112}Sn were proposed as nuclei close to the critical point.

The sextic oscillator model was developed further in Ref. [22], where the exact analytic formalism was extended to $M = 2$, i.e., to a higher degree of the QES solution. In this case, the roots of a cubic algebraic equation had to be calculated (see the discussion in Section 2.2). The considerably larger model space (30 states compared to 10) allowed for a more elaborate comparison with the experimental data but also raised new questions. The enlarged basis included the ground-state band (up to $L^\pi = 10^+$); states that could be assigned to a $K^\pi = 2^+$ band (up to $L^\pi = 8^+$); and three excited 0^+ states, which act as bandheads. Two of them were analogous to those appearing in the simple version of the model ($(\xi, \tau)L = (1, 3)0$ and (2,0)0), whereas the (3,0)0 state was a higher nodally excited configuration. Identifying the experimental counterpart of the excited 0^+ states remained the key step in the application of the extended model.

Furthermore, a new question arose. In the original version of the model [20,21], the states belonging to the same (ξ, τ) multiplet were considered degenerate in energy. The pattern of states with larger L values appearing in the extended model revealed that the spectrum did not follow this degeneracy; rather, typically, the levels with higher L appeared higher in the spectrum. For this reason, in Ref. [22], the Hamiltonian was extended by a phenomenological rotational term $cL \cdot L$. The justification for this rotational term was presented in Ref. [22].

In the first application of the extended model [22], the Ru and Pd chains were revisited. With the larger M, the c^π numbers (in Equation (12)) also changed ($c^+ = 15/4$ was used instead of $11/4$), which slightly modified the location of the critical parabola. The conclusions for the Ru chain were essentially the same as in the limited model: the critical point was again close to ^{104}Ru. The situation was somewhat different for the Pd chain, perhaps due to the enlarged model space and the rotational term. Most of the Pd nuclei were located in the domain of the spherical minimum (below the critical parabola); however, ^{108}Pd, which had a rich enough collection of $B(E2)$ values for comparison with the experiment, showed marked signs of a critical-point nucleus. The results for the energies and B(E2) in ^{108}Pd are shown in Figure 4. Besides this nucleus, ^{110}Pd was also found to be located close to the critical parabola.

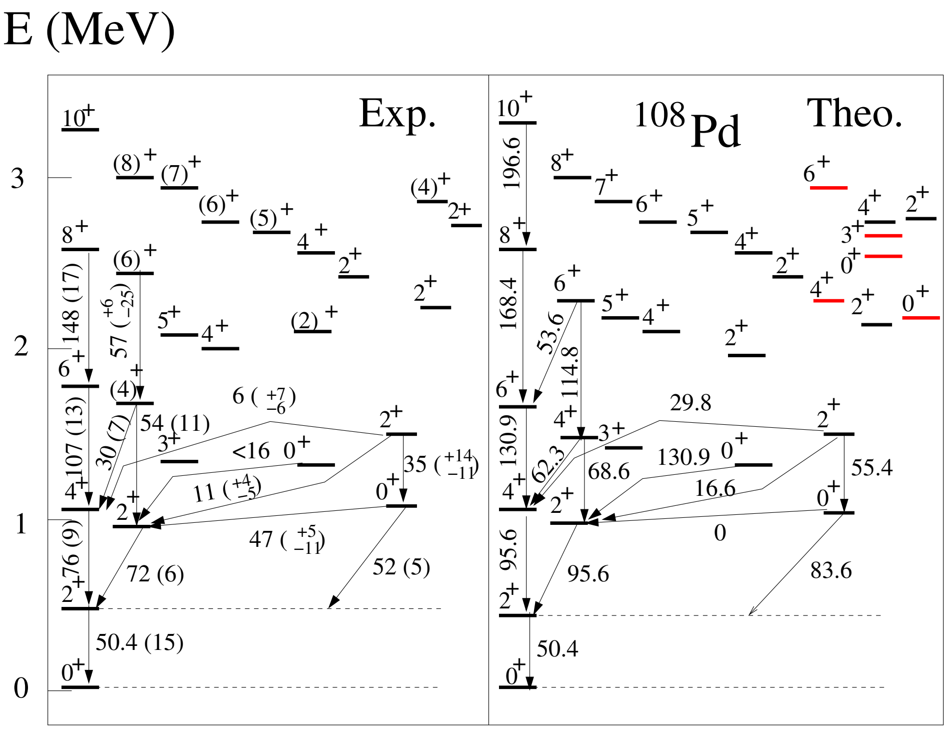

Figure 4. Experimental and calculated energy spectrum, as well as B(E2) transitions, for the ^{108}Pd nucleus using the sextic oscillator. Theoretical E2 transitions are normalized to the experimental value B(E2; $2_1^+ \to 0_1^+$) = 50.4 W.u. Theoretical energy levels indicated in red are predicted ξ= 2 and 3 levels without experimentally assigned partners. The figure was taken from Ref. [22] and is licensed under CC BY-SA 4.0.

In the next application [23] of the extended model, Pt and Os nuclei were studied close to the closure of the $Z = 82$ shell. A thorough analysis of the decay pattern of the excited 0^+ states was carried out in order to assign the model states to their experimental counterparts. It was found that the members of the node-excited band built on the $(\xi, \tau)0 = (2, 0)0$ state systematically became lower with increasing A, and eventually, the (2,0)0 bandhead state fell below the (1,3)0 bandhead state for ^{198}Pt. This is shown in Figure 5.

This change was accompanied by a drastic change in the potential shape, indicating the realization of the phase transition from the γ-unstable to the spherical domain. Similar trends were also observed for the Os chain. However, the last isotope with a reasonably comprehensive spectroscopic data set, ^{192}Os, remained clearly in the domain of a γ-unstable deformed shape. Indirect signs indicated that the shape-phase transition could occur near ^{194}Os, but the spectroscopic information was insufficient to prove this unambiguously. This study also confirmed that ^{194}Pt and ^{196}Pt were rather good examples of the γ-unstable configuration (see Figure 6, taken from Ref. [23]), whereas this was less pronounced for the Os isotopes, which, especially the lighter ones, showed signs of a triaxial configuration.

There have been further studies estimating the performance of the sextic oscillator as a β potential by abandoning exact solutions. In Ref. [32], higher QES solutions were considered using numerical calculations. A comparison with a large array of experimental spectroscopic data for the nuclei discussed in Ref. [21] indicated that the order $k = 2$ seems to be the optimal choice in most calculations. This corresponds to $M = 2$, i.e., the extended scheme with M up to 2 presented in Refs. [22,23], providing strong support for this fully analytical model.

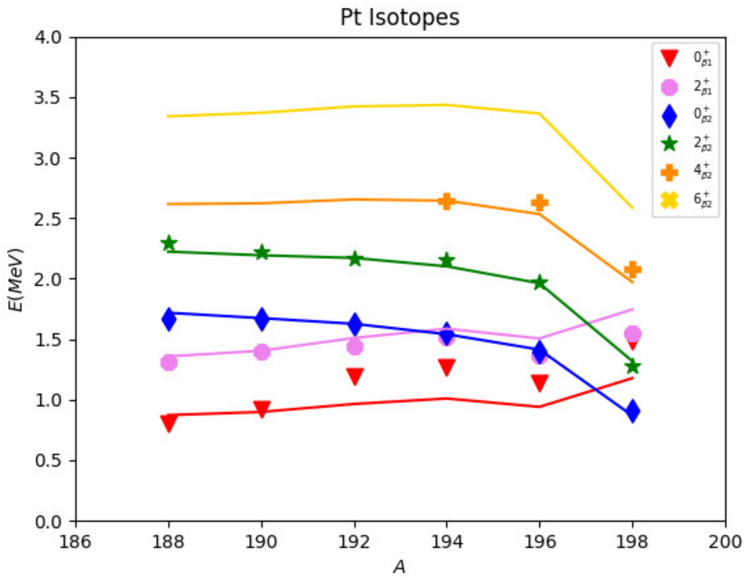

Figure 5. First low-lying systematics for the lowest excited $K^\pi = 0^+$ bands for the Pt isotopes. Lines indicate the theoretical levels: $(\xi, \tau)L = (1,3)0$ and $(1,4)2$ for the first band, and $(2,0)0$, $(2,1)2$, $(2,2)4$, and $(2,3)6$ for the second one. Experimental data are indicated by symbols of the same color. The figure was taken from Ref. [23] and is licensed under CC BY-SA 4.0.

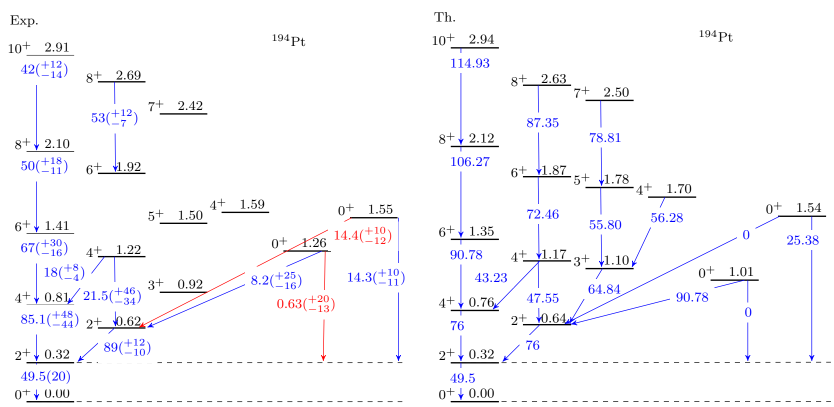

Figure 6. The experimental and theoretical energy (in MeV) spectrum of ^{194}Pt with $E2$ transitions. Transitions predicted to be forbidden in the model are indicated in red in the experimental (**left**) panel. The figure was taken from Ref. [23] and is licensed under CC BY-SA 4.0.

Ref. [42] focused on an alternative approach to addressing the problem of degeneracies in the sextic oscillator model. This problem was addressed in Refs. [22,23] by directly introducing a phenomenologic rotational term in the Hamiltonian. In Ref. [42], a rotational term $L(L+1)/\beta^2$ was directly incorporated into the $u(\beta)$ potential to resolve the degeneracy of the multiplets. Numerical methods were used to calculate the spectroscopic quantities, and the model was used to reproduce experimental data for a number of Xe isotopes. The results showed good agreement with the data, especially in the case of the staggering pattern appearing in the quasi-γ bands.

3.2. $w(\gamma)$ Non-Zero

As discussed in Section 2, exact solutions for a $v(\beta, \gamma)$ potential can be obtained if the potential can be separated into $u(\beta)$ and $w(\gamma)$ components. This requires certain assumptions and approximations. To obtain a solvable problem in the γ variable, further approximations are necessary. Generally, it is assumed that $w(\gamma)$ has a minimum at either $\gamma = 0$ or $\gamma = \pi/6$, and the potential is expanded around these minima. The two choices lead to different solutions and different physical systems, i.e., different nuclear shape configurations.

When the expansion of $w(\gamma)$ is carried out around $\gamma = 0$, the Bohr Hamiltonian describes nuclear shapes that evolve from an axially symmetric shape to a triaxial one. By combining this system with a $u(\beta)$ potential that allows a spherical or deformed minimum, phase transitions from the spherical to the axially deformed shapes can be described with an $X(5)$ critical-point symmetry [7]. A key development in this area was presented in Ref. [27], where the sextic oscillator was used as $u(\beta)$, while the γ potential was defined as $w(\gamma) = w_1 \cos(3\gamma) + w_2 \cos^2(3\gamma)$. With an appropriate variable change, the solutions of the differential equation obtained for the γ component were written in terms of the spheroidal functions. This model was coined the sextic and spheroidal approach (SSA) and was later also referred to as $X(5)$-sextic. Calculations were carried out for nuclei typically considered candidates for the $X(5)$ symmetry: Os ($A = 176$–180, 188–190), ^{150}Nd, ^{156}Dy, and Hf ($A = 166$–68). The predictions were compared to those of alternative models with different $u(\beta)$ used in the Bohr Hamiltonian, i.e., the infinite square well (ISW) and the Davidson (D) potential, and also to those of the coherent state model (CSM), which is based on a boson operator formalism. It was found that the best agreement with the experimental energy eigenvalues was found for the D, SSA, and CSM models, whereas for the $B(E2)$ values, the SSA and the CSM performed slightly better. Among the nuclei considered, ^{188}Os was found to come closest to the critical point of the phase transition.

By applying the expansion of the $w(\gamma)$ around $\gamma = \pi/6$, transitions between the prolate and oblate shape phases can be described, and the corresponding critical-point solution is $Z(5)$ [9]. The sextic oscillator was applied in this setting as a $u(\beta)$, while the γ potential was defined as $w(\gamma) = \mu \cos^2(3\gamma)$ [26]. Solutions to the differential equation of the γ component were obtained after transforming the latter into the Mathieu equation. This model was referred to as the sextic and Mathieu approach (SMA) or $Z(5)$-sextic. Predictions of the model were calculated for five isotopes—^{188}Os, ^{190}Os, ^{192}Os, ^{228}Th, and ^{230}Th—which partially overlap with the examples studied in the $X(5)$-sextic model. Since transitions among well-deformed nuclei (from prolate to oblate) through a triaxial critical point were studied, regions where this transition was expected, such as Os and Th isotopes, were considered. Predictions for the energy spectrum and the electric quadrupole transitions in the ground, γ, and β bands were compared to the experimental values, as well as to the results obtained from the coherent state model (CSM). Signatures for triaxiality were analyzed in the energy spectra. Reasonable agreement was found between the experimental and the SMA and CSM values. A similar analysis (with similar results) was carried out for the nuclei ^{180}Hf and ^{182}W [43]. Besides the application of the SMA to certain nuclei, this work also focused on exploring the relation between the SMA and the CSM. It was found that the SMA formalism could be obtained by quantizing the classical CSM equations, and the SMA represented the strong coupling limit of the CSM.

3.3. The γ-Rigid Cases

A special kind of solvability arises when the γ variable is "frozen" to some value, typically $\gamma = 0$ or $\gamma = \pi/6$, i.e., the minimum values of $w(\gamma)$ in the $X(5)$ and $Z(5)$ models. This ensures the separation of variables while reducing the number of active variables.

As described in Section 2.1, when $\gamma = 0$, the $X(5)$ model reduces to $X(3)$—the model that can account for axially symmetric γ-rigid shapes. Combining this with the sextic oscillator as $u(\beta)$, the $X(3)$-sextic model arises [29]. Predictions for some characteristic energy ratios were calculated, and compared to the corresponding values obtained for polynomial versions of the $X(3)$ model: $X(3)$, $X(3)$-β^2, $X(3)$-β^4, and $X(3)$-β^6. A simplified version of this model, without a quartic term, was considered in Ref. [44] and compared to the same models. The energy spectrum of the ground and the first two excited β bands was numerically calculated for a large number of nuclei: Ru ($A = 98$–108), Mo ($A = 100$, 102), Xe ($A = 116$–130), Ce ($A = 132$, 134), Nd ($A = 146$–150), Sm ($A = 150$, 152), Gd ($A = 152$, 154), Dy ($A = 154$, 156), ^{172}Os, Pt ($A = 180$–196), ^{190}Hg, and ^{222}Ra. The energy eigenvalues and $B(E2)$ ratios were reproduced reasonably well. A first-order shape-phase transition between a γ-rigid prolate harmonic vibrator and γ-rigid prolate anharmonic vibrator was identified, and candidates for the corresponding critical point were proposed. The best candidates were found to be ^{104}Ru, ^{120}Xe, ^{126}Xe, and ^{148}Nd, while ^{128}Xe, ^{172}Os, and ^{196}Pt were also close to the critical point. We note that ^{104}Ru was also considered a critical-point nucleus in the spherical to γ-unstable shape-phase transition, i.e., in the $E(5)$-sextic model.

The $X(3)$-sextic model has been further developed along several lines. In Ref. [45], the minimal length (ML) formalism was incorporated into the model, whereas in Ref. [46], the deformation-dependent mass (DDM) formalism was considered. As a further option, in Ref. [47], the order of the QES solutions was varied, and the results were compared. Calculations were carried out in all three studies for the same set of nuclei as discussed in Ref. [29]. The quality of the fits was generally improved due to the extra parameters, but the conclusions concerning the critical-point nuclei essentially remained the same.

Another γ-rigid model can be obtained from $Z(5)$-sextic by fixing γ to $\pi/6$ [28], leading to $Z(4)$-sextic. In this case, exact solutions could be obtained for the ground and the β bands, whereas for the γ band, approximations had to be applied. Numerical calculations were carried out for the Xe ($A = 128$-132) and Pt ($A = 192$-196) nuclei. The results for the energy spectrum and the $B(E2)$ transitions were compared to the experimental values, as well as to the predictions of the $Z(4)$ model. Qualitative agreement of the data sets was found, and a shape-phase transition was identified near ^{130}Xe, where a deformed minimum gave way to a spherical one. It is notable that these regions were also identified as candidates for phase transition in the $E(5)$ and $X(3)$ models.

3.4. Unrestricted Sextic Oscillator

The QES formalism restricts the parameters of the sextic oscillator, meaning that the allowed potential shapes are also restricted. It is known, for example, in [20–22], that in the case of a double-well structure (left of the critical parabola in Figure 2), the deformed minimum is always deeper than the spherical one. Double-well structures different from this one can be studied for the general sextic oscillator; however, in this case, the exact analytical calculations have to be replaced with numerical approaches.

In Ref. [31], the general double-well sextic potential was used as a β potential to describe γ-unstable nuclei. The model states were constructed using a numerical diagonalization procedure in a basis classified by the $E(5) \supset SO(5) \supset SO(3) \supset SO(2)$ group chain. The model parameters were determined by fitting the low-lying energy spectra of Mo isotopes ($A = 96$, 98, and 100). Reasonable agreement was found between the theoretical and experimental energy eigenvalues. The difference between the energy minima showed a decreasing trend with an increasing mass number, similar to the height of the potential barrier between the minima. The $B(E2)$ values calculated with the resulting wave functions also showed reasonable agreement with the experimental values. ^{100}Mo was found to exhibit properties expected near the critical point.

A similar study was carried out in Ref. [48] within the $X(5)$ formalism to describe the first-order phase transition between spherical and axially deformed nuclear shapes. The β potential was a one-parameter double-well sextic oscillator with two degenerate minima (one spherical and one deformed). The calculated spectrum, as a function of the free parameter, exhibited predictions in accordance with the $SU(3)$ and $X(5)$-β^6 models in certain limits of the parameter. Depending on the relative energy of the barrier compared to the low-energy states, the study identified cases of coexisting shapes in the ground state and the 0^+ β-excited state. The paper discussed critical situations of shape coexistence from a phenomenological perspective, employing the density of probability distribution for the deformation and $E0$ transitions. Experimental evidence supporting these critical phenomena was mentioned for a few selected nuclei (^{152}Nd, ^{170}Hf, and ^{238}Pu). Similar critical potentials with shape coexistence are expected for higher excited states. In addition, in Ref. [49], along the same lines, the sextic potential was used to show the connections between shape coexistence and shape transitions.

Lastly, it is worth highlighting the connection between the sextic potential and Catastrophe Theory (CT) [50]. This theory provides a framework for understanding abrupt transitions in various natural and artificial systems. It offers a unique perspective on the dynamics of complex systems and the potential for abrupt, transformative changes within them. CT is relevant in multiple fields, including science, economics, psychology, engineering, ecology, etc. Specifically, the sextic potential is associated with the A_{+5} butterfly catastrophe, whose germ is represented by the function x^6. In this context, the potential used is typically expressed as $u(\beta) = \beta^6 + a_4\beta^4 + a_2\beta^2$, where a_2 and a_4 are free parameters. Importantly, for γ-independent potentials, this setup not only accounts for transitions from spherical to deformed shapes through a second-order phase transition but also accommodates the critical point at which the minima corresponding to spherical and deformed shapes become degenerate, giving rise to a first-order phase transition. In a recent publication [51], this relationship was explored within the context of an algebraic approach, leading to the derivation of the general phase diagram for the butterfly catastrophe. This comprehensive phase diagram includes analytical expressions for key features such as the tricritical point, the critical lines for both first- and second-order transitions, and additionally, the delineation of spinodal and anti-spinodal lines that demarcate the regions of coexistence between spherical and deformed shapes. This connection to Catastrophe Theory provides valuable insights into the complex dynamics of nuclear shape transitions.

3.5. Further Generalizations

The sextic oscillator is not the only quasi-exactly solvable potential. In fact, polynomial potentials of degree $4\nu + 2$ belong to this class. Following the sextic oscillator ($\nu = 1$), the decadic oscillator ($\nu = 2$) also admits similar mathematical formalism. The coefficients of the potential terms also obey certain constraints. In Ref. [52], the decadic oscillator was employed to describe nuclei that were supposed to lie near the $E(5)$ critical point, characterizing the phase transition from the spherical to the γ-unstable shape phases. The spectroscopic results were compared to the experimental data and the results obtained from various models ($E(5)$, $E(5)$-sextic, etc.). It was found that the quality of the fit to the experimental energy eigenvalues (in terms of χ^2) was better for the sextic oscillator and the decadic oscillator for three and two nuclei, respectively (^{102}Pd, ^{104}Ru, and ^{116}Cd vs. ^{114}Cd and ^{134}Ba), whereas it was of similar quality for one case (^{108}Pd). In the case of six Xe isotopes, the performance of the decadic oscillator was better for four nuclei. In all cases, both models performed better than the original $E(5)$ model based on the infinite square as well as $u(\beta)$. However, for the $B(E2)$ ratios, the $E(5)$ model almost always performed best, and the sextic oscillator was the worst. This may be due to the difference in the asymptotic tail of the wave functions. It is important to note that higher-order polynomial potentials lead to more intricate recurrence relations and, consequently, more complex truncation conditions. Exact analytical solutions for such potentials cannot be attained as straightforwardly, as demonstrated in Equation (12). This significantly reduces the number of algebraic analytical solutions. With regard to these exact solutions, due to the intricacies involved in truncating the series expansion, interested readers should be mindful of the complications outlined in Ref. [53].

Another generalization of the sextic oscillator was discussed in Ref. [54]. The authors discussed odd-A nuclei in the γ-soft region in a model where the $E(5)$-sextic Hamiltonian is combined with a single nucleon on a $j = 3/2$ orbit. In the resulting $E(5/4)$ model, the single-particle features are represented by a five-dimensional spin–orbit interaction and an angular momentum degeneracy-breaking term proportional to $J(J+1)$. The energy spectrum and the $B(E2)$ rates were precisely calculated for odd Ir isotopes with $A = 187$ to 195. Good agreement was found between the experimental data and the model predictions.

4. Summary and Conclusions

In summary, we have provided an overview of recent research into the phase transitional behavior exhibited by the equilibrium shapes of atomic nuclei. Our exploration is based on the Bohr equation and its solutions using simple potentials. We revised and briefly proposed critical-point solutions (CPSs) linked to the use of an infinite square well for the β variable and various selections for the γ degree of freedom: E(5), X(5), Z(5), X(3), and Z(4). These simple CPSs shed light on the structural properties at the phase transitional point. Then, extensions and alternatives to CPSs by substituting the infinite square well in β with a sextic potential were revised, offering valuable insights into their relevance and accuracy. These studies outline the broader landscape of possibilities in understanding structural evolution within atomic nuclei. This exploration opens up the prospect of a fresh perspective on the intricate journey of nuclear structure evolution, marking a promising avenue for future research in the field.

Figure 7 displays the region of the nuclide chart where models based on the sextic oscillator have been applied in the Bohr Hamiltonian. Only even-even nuclei are shown, indicating the models in terms of which the given nucleus has been discussed (using both exact and numerical methods) in any of the works reviewed here. The $E(5)$-sextic model, describing the transition from the spherical to the γ-unstable shape phase, is applied on both sides of the $Z = 50$ shell closure and to nuclei near the lower side of the $Z = 82$ shell closure. The spherical phase appears close to the $N = 50$ shell closure for nuclei with $Z < 50$, the $N = 82$ shell closure for $Z > 50$, and the $N = 126$ shell closure for $Z < 82$. The $X(5)$ model accounting for the transition from spherical to axially deformed shape phase in regions further away from shell closures has been applied to nuclei with $N > 82$ and $Z < 82$. The γ-rigid version of this model, $X(3)$, has been applied more extensively in this region and also on both sides of the $Z = 50$ shell closure. Frequently, the same nuclei have been discussed in terms of the $X(3)$ and $E(5)$ frameworks. The $Z(5)$ model, describing the transition between prolate and oblate shape phases, has been applied to a few nuclei further away from the shell closures with $Z < 82$ and $N < 126$. Its γ-rigid limit has been applied close to this region and also near the domain near the shell closures with $Z > 50$ and $N < 82$. There are a few nuclei that have been discussed in terms of three models simultaneously (^{128}Xe, ^{130}Xe, ^{192}Pt, ^{194}Pt, and ^{196}Pt: $E(5)$, $X(3)$, and $Z(4)$; ^{188}Os and ^{190}Os: $E(5)$; and $X(5)$ and $Z(5)$).

Transitions between nuclear shapes through critical points are also displayed in Figure 7 in the models reviewed here. A simple pattern (diagonal lines formed by triangles) seems to emerge for the critical-point nuclei in the $E(5)$-sextic model on both sides of the $Z = 50$ shell closure. These nuclei separate the region of spherical nuclei close to shell closures from that of gamma-unstable nuclei somewhat further away. Regions associated with the other models are not extensive enough to identify similar systematics.

In conclusion, it is crucial to underscore that the incorporation of a sextic potential into the Bohr–Mottelson model provides a unique avenue for investigating the evolution of nuclear shapes across the entire nuclide chart. Within this framework, quasi-exact solutions hold substantial significance, serving as a pivotal milestone and reference point for any prospective numerical solutions aimed at comprehensively characterizing the broader landscape of the sextic potential's influence on nuclear shapes.

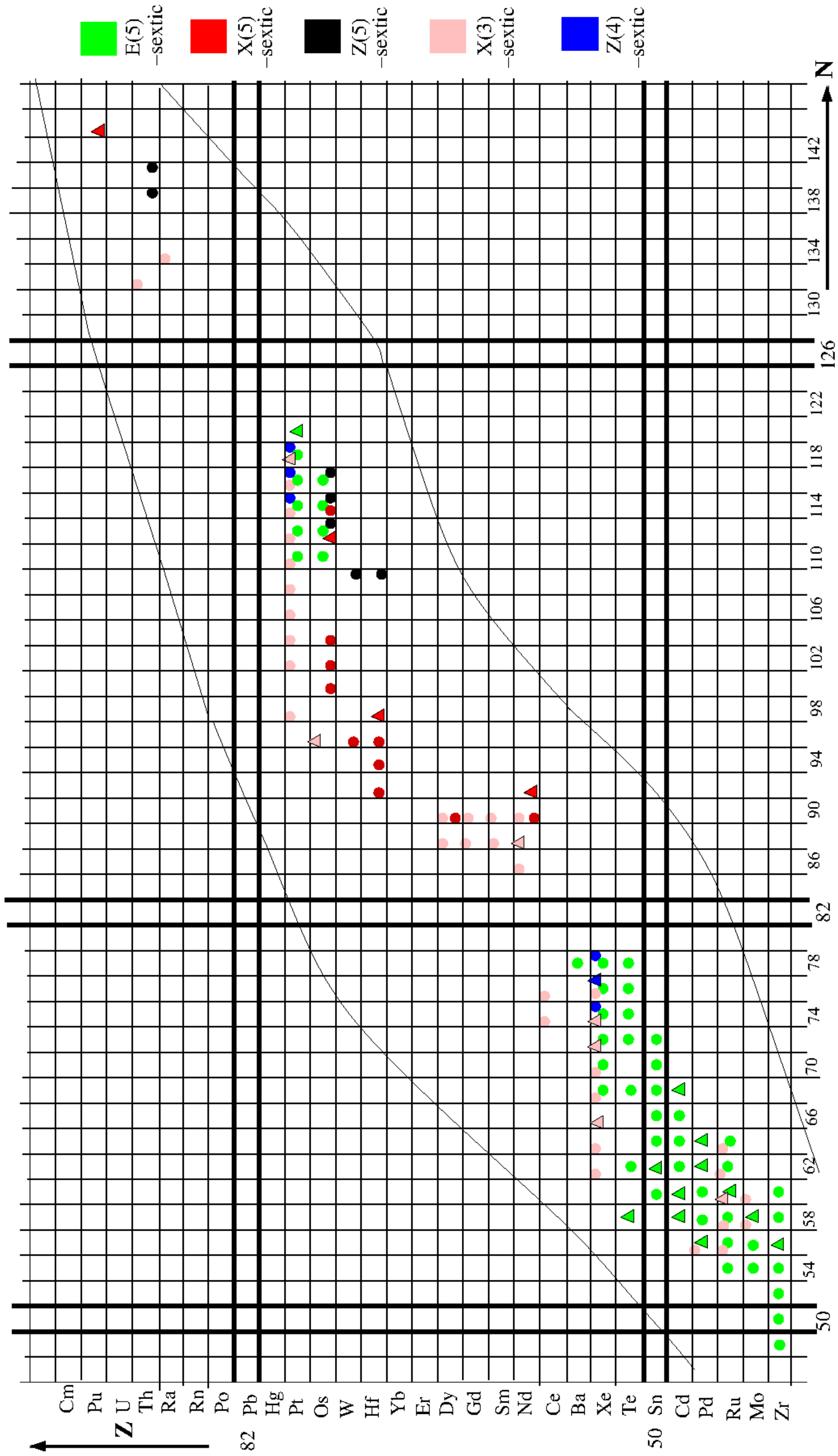

Figure 7. Even-even nuclei in terms of various models utilizing the sextic oscillator as $u(\beta)$. The color and position of the dots inside the boxes identify the models: $E(5)$-sextic: green dot in the middle; $X(5)$-sextic: red dot in the lower-left corner; $Z(5)$-sextic: black dot in the lower-right corner; $X(3)$-sextic: pink dot in the upper-left corner; $Z(4)$-sextic: blue dot in the upper-right corner. Nuclei proposed as critical are marked with a triangle (instead of a dot).

Author Contributions: All authors contributed equally to this review article. They have read and agreed to the published version of the manuscript.

Funding: This work was partially supported by the Consejería de Economía, Conocimiento, Empresas y Universidad de la Junta de Andalucía (Spain) under Group FQM-160, under Projects No. P20-01247 and No. US-1380840, and also through Projects No. PID2019-104002GB-C22, No. PID2020-114687GB-I00, and No. PID2022-136228NB-C22 funded by MCIN/AEI/10.13039/50110001103 and "ERDF A way of making Europe". This work was supported by the National Research, Development and Innovation Office (NKFIH, Hungary), Grant No. K128729.

Data Availability Statement: Not applicable.

Conflicts of Interest: The authors declare no conflict of interest.

References

1. Landau, L.D.; Lifshitz, E.M. *Statistical Physics*; Pergamon Press: Oxford, UK, 1969.
2. Iachello, F.; Zamfir, N.V. Quantum Phase Transitions in Mesoscopic Systems. *Phys. Rev. Lett.* **2004**, *92*, 212501. [CrossRef] [PubMed]
3. Sachdev, S. *Quantum Phase Transitions*; Cambridge University Press: Cambridge, UK, 1999.
4. Carr, L. *Understanding Quantum Phase Transitions*; CRC Press: Boca Raton, FL, USA, 2011.
5. Bohr, A.; Mottelson, B. *Nuclear Structure*; Benjamin: Reading, MA, USA, 1975; Volume 2.
6. Iachello, F. Dynamic Symmetries at the critical point. *Phys. Rev. Lett.* **2000**, *85*, 3580–3583. [CrossRef] [PubMed]
7. Iachello, F. Analytic description of critical point nuclei in a spherical-axially deformed shape phase transition. *Phys. Rev. Lett.* **2001**, *87*, 052502. [CrossRef] [PubMed]
8. Iachello, F. Phase Transitions in Angle Variables. *Phys. Rev. Lett.* **2003**, *91*, 132502. [CrossRef]
9. Bonatsos, D.; Lenis, D.; Petrellis, D.; Terziev, P.A. Z(5): Critical point symmetry for the prolate to oblate nuclear shape phase transition. *Phys. Lett. B* **2004**, *588*, 172–179. [CrossRef]
10. Iachello, F.; Arima, A. *The Interacting Boson Model*; Cambridge University: New York, NY, USA, 1987.
11. Ginocchio, J.N.; Kirson, M.W. An intrinsic state for the interacting boson model and its relationship to the Bohr-Motelson model. *Nucl. Phys. A* **1980**, *350*, 31–60. [CrossRef]
12. Ginocchio, J.N.; Kirson, M.W. Relationship between the Bohr collective Hamiltonian and the interacting-boson model. *Phys. Rev. Lett.* **1980**, *44*, 1744–1747. [CrossRef]
13. Dieperink, A.E.L.; Scholten, O.; Iachello, F. Classical limit of the interacting-boson model. *Phys. Rev. Lett.* **1980**, *44*, 1747–1750. [CrossRef]
14. Casten, R.F. Shape phase transitions and critical-point phenomena in atomic nuclei. *Nat. Phys.* **2006**, *2*, 811–820. [CrossRef]
15. Casten, R.F.; Cutchan, E.A.M. Quantum phase transitions and structural evolution in nuclei. *J. Phys. G Nucl. Part. Phys.* **2007**, *34*, R285–R320. [CrossRef]
16. Casten, R.F. Quantum phase transitions and structural evolution in nuclei. *Prog. Part. Nucl. Phys.* **2009**, *62*, 183–209. [CrossRef]
17. Cejnar, P.; Jolie, J. Quantum phase transitions in the interacting boson model. *Prog. Part. Nucl. Phys.* **2009**, *62*, 210–256. [CrossRef]
18. Cejnar, P.; Jolie, J.; Casten, R.F. Quantum phase transitions in the shapes of atomic nuclei. *Rev. Mod. Phys.* **2010**, *82*, 2155–2212. [CrossRef]
19. Fortunato, L. Solutions of the Bohr Hamiltonian, a compendium. *Eur. Phys. J. A* **2005**, *26*, 1. [CrossRef]
20. Lévai, G.; Arias, J.M. The sextic oscillator as a $\gamma-$independent potential. *Phys. Rev. C* **2004**, *69*, 014304. [CrossRef]
21. Lévai, G.; Arias, J.M. Search for critical-point nuclei in terms of the sextic oscillator. *Phys. Rev. C* **2010**, *81*, 044304. [CrossRef]
22. Lévai, G.; Arias, J.M. Extended analytical solutions of the Bohr Hamiltonian with the sextic oscillator. *J. Phys. G Nucl. Part. Phys.* **2021**, *48*, 085102. [CrossRef]
23. Baid, S.; Lévai, G.; Arias, J.M. Extended analytical solutions of the Bohr Hamiltonian with the sextic oscillator: Pt-Os isotopes. *J. Phys. G Nucl. Part. Phys.* **2023**, *50*, 045104. [CrossRef]
24. Ushveridze, A.G. *Quasi-Exactly Solvable Models in Quantum Mechanics*; Institute of Physics Publishing: Bristol, UK, 1994.
25. Turbiner, A.V. One-dimensional quasi-exactly solvable Schrödinger equations. *Phys. Rep.* **2016**, *642*, 1. [CrossRef]
26. Raduta, A.A.; Buganu, P. Toward a new description of triaxial nuclei. *Phys. Rev. C* **2011**, *83*, 034313. [CrossRef]
27. Raduta, A.A.; Buganu, P. Application of the sextic oscillator with a centrifugal barrier and the spheroidal equation for some $X(5)$ candidate nuclei. *J. Phys. G* **2013**, *40*, 025108. [CrossRef]
28. Buganu, P.; Budaca, R. Analytical solution for the Davydov-Chaban Hamiltonian with a sextic potential for $\gamma = 30^{\circ}$. *Phys. Rev. C* **2015**, *91*, 014306. [CrossRef]
29. Buganu, P.; Budaca, R. Sextic potential for $\gamma-$rigid prolate nuclei. *J. Phys. G* **2015**, *42*, 105106. [CrossRef]
30. Budaca, R.; Buganu, P.; Chabab, M.; Lahbas, A.; Oulne, M. Extended study on a quasi-exact solution of the Bohr Hamiltonian. *Ann. Phys.* **2016**, *375*, 65. [CrossRef]
31. Budaca, R.; Budaca, A.I.; Buganu, P. Application of the Bohr Hamiltonian with a double-well sextic potential to collective states in Mo isotopes. *J. Phys. G Nucl. Part. Phys.* **2019**, *46*, 125102. [CrossRef]
32. Lahbas, A.; Buganu, P.; Budaca, R. Quasi-exact description of the γ-unstable shape phase transition. *Mod. Phys. Lett. A* **2020**, *35*, 2050085. [CrossRef]
33. Wilets, L.; Jean, M. Surface Oscillations in Even-Even Nuclei. *Phys. Rev.* **1956**, *102*, 788. [CrossRef]

34. Davydov, A.S.; Chaban, A.A. Rotation-vibration interaction in non-axial even nuclei. *Nucl. Phys.* **1960**, *20*, 499. [CrossRef]
35. Bonatsos, D.; Lenis, D.; Petrellis, D.; Terziev, P.A.; Yigitoglu, I. $X(3)$: An exactly separable $\gamma-$rigid version of the $X(5)$ critical point symmetry. *Phys. Lett. B* **2006**, *632*, 238–242. [CrossRef]
36. Meyer-ter-Vehn, J. Collective model description of transitional odd-A nuclei: (I). The triaxial-rotor-plus-particle model. *Nucl. Phys. A* **1975**, *249*, 111. [CrossRef]
37. Bonatsos, D.; Lenis, D.; Petrellis, D.; Terziev, P.A.; Yigitoglu, I. $\gamma-$rigid solution of the Bohr Hamiltonian for $\gamma = 30°$ compared to the E(5) critical point symmetry. *Phys. Lett. B* **2005**, *621*, 102–108. [CrossRef]
38. Ishkhanyan, A.M.; Lévai, G. Hermite function solutions of the Schrödinger equation for the sextic oscillator. *Phys. Scr.* **2020**, *95*, 085202. [CrossRef]
39. Buganu, P.; Fortunato, L. Recent approaches to quadrupole collectivity: Models, solutions and applications based on the Bohr hamiltonian. *J. Phys. G Nucl. Part. Phys.* **2016**, *43*, 093003. [CrossRef]
40. Kharb, S.; Chand, F. Searching Critical-Point Nuclei in Te- and Xe-Isotopic Chains Using Sextic Oscillator Potential. *Phys. At. Nucl.* **2012**, *75*, 168–172. [CrossRef]
41. Kumar, V.; Bhardwaj, S.B.; Singh, R.M.; Chand, F. Energy eigenvalue spectra and applications of the sextic and the Coulomb perturbed potentials. *Phys. Scr.* **2022**, *97*, 055301. [CrossRef]
42. Hassanabadi, H.; Sobhani, H. Elimination of degeneracy in the *gamma*-unstable Bohr Hamiltonian in the presence of an extended sextic potential. *Phys. Rev. C* **2018**, *98*, 014312. [CrossRef]
43. Raduta, P.B.A.A.; Faessler, A. New features of the triaxial nuclei described with a coherent state model. *J. Phys. G Nucl. Part. Phys.* **2012**, *39*, 025103.
44. Budaca, R. Harmonic oscillator potential with a sextic anharmonicity in the prolate γ-rigid collective geometrical model. *Phys. Lett. B* **2014**, *739*, 56. [CrossRef]
45. Batoul, A.E.; Oulne, M.; Tagdamte, I. Collective states of even-even nuclei in γ-rigid quadrupole Hamiltonian with minimal length under the sextic potential. *J. Phys. G Nucl. Part. Phys.* **2021**, *48*, 085106. [CrossRef]
46. Oulne, M.; Tagdamte, I. Bohr Hamiltonian with sextic potential for γ-rigid prolate nuclei with deformation-dependent mass term. *Phys. Rev. C* **2022**, *106*, 064313. [CrossRef]
47. Oulne, M.; Tagdamte, I. Extended study on the application of the sextic potential in the frame of X(3)-sextic. *J. Phys. G: Nucl. Part. Phys.* **2022**, *49*, 035102. [CrossRef]
48. Budaca, R.; Buganu, P.; Budaca, A.I. Bohr model description of the critical point for the first order shape phase transition. *Phys. Lett. B* **2018**, *776*, 26–31. [CrossRef]
49. Budaca, R.; Budaca, A.I. Coexistence, mixing and fluctuation of nuclear shapes. *Europhys. Lett.* **2018**, *123*, 42001. [CrossRef]
50. Gilmore, R. *Catastrophe Theory for Scientists and Engineers*; John Wiley & Sons: New York, NY, USA, 1981.
51. Leviatan, A.; Gabrielov, N. Quantum Catastrophes from an Algebraic Perspective. *J. Phys. Conf. Ser.* **2020**, *1612*, 012020. [CrossRef]
52. Sobhani, H.; Hassanabadi, H.; Bonatsos, D.; Pan, F.; Cui, S.; Fen, Z.; Draayer, J.P. Analytical study of the γ-unstable Bohr Hamiltonian with quasi-exactly solvable decatic potential. *Eur. Phys. J. A* **2020**, *56*, 29. [CrossRef]
53. Amore, P.; Fernández, F.M. On some conditionally solvable quantum-mechanical problems. *Phys. Scr.* **2020**, *95*, 105201. [CrossRef]
54. Sobhani, H.; Hassanabadi, H.; Bonatsos, D.; Pan, F.; Draayer, J.P. γ-unstable Bohr Hamiltonian with sextic potential for odd-A nuclei. *Nucl. Phys. A* **2020**, *1002*, 121956. [CrossRef]